POWER FLOW CONTROL IN HYBRID ELECTRIC VEHICLES

Guillermo Becerra
Instituto de Ingeniería
Universidad Nacional Autónoma de México
México, DF. 04510
México
Email: guillermobec@gmail.com

José Luis Mendoza-Soto
Luis Alvarez-Icaza
Instituto de Ingeniería
Universidad Nacional Autónoma de México
México, DF. 04510
México
Email: jmendozas@ii.unam.mx
Email: alvar@pumas.iingen.unam.mx

ABSTRACT

In this paper a new strategy for controlling the power flow in hybrid electric vehicles is described. The strategy focuses in the planetary gear system where kinematic and dynamic constraints must be satisfied. The aim is to satisfy driver demands and to reduce fuel consumption. The resultant power flow control is continuos and uses the internal combustion engine with the maximum possible efficiency. The strategy is not optimal, although it is inspired by the solution to most optimization problems. The main advantages are that the computational cost is low, when compared to optimization based approaches, and that it is easy to tune. The strategy is tested with simulations using a mathematical model of a power train of a hybrid diesel-electric bus subjected to the power demands of representative urban area driving cycles. Simulation results indicate that the strategy achieves small speed tracking errors and attains good fuel consumption reduction levels.

INTRODUCTION

In recent years, peaking of oil production, causing its price to rise, and growing concerns of environmental impact of human activity are pushing the development of solutions for a more efficient use of energy. In transportation, reductions on fossil fuel consumption are sought by the use of technologies like hybrid electric vehicles (HEV) and the use of fuels obtained from renewable energy sources. This paper focuses on the design of a power flow control strategy for a HEV composed by a diesel internal combustion engine and an electric induction machine. HEV may have different architectures that require the use of diverse energy management strategies. The main architectures, as presented in [1], are series, parallel or series-parallel. A key component for power control in the last two architectures is the Continuosly Variable Transmission (CVT). A comparison of the architectures is presented in [2].

Power distribution in HEV can be performed by the use of different controllers, as described in the comparative study of supervisory control strategies for HEV presented in [3]. Chau and Chan [4] show some important details of the integrated starter-generator (ISG) and propulsion systems with a CVT. Xiong et al [5] propose a fuzzy logic control for energy management. Tzeng et al [6] apply fuzzy logic control for energy manegement in a HEV of parallel configuration with a pulley-belt CVT. Xiong and Yin [7] present a fuzzy logic controller for energy management of a series-parallel hybrid electric bus with ISG. In most of these revised cases, strategies are based on a set of rules for each one of the driving modes in HEV [3].

There are also power flow control strategies based on optimization, like those revised in [3]. They are normally not implemented in real time and their off-line optimization results are used with a look-up table. Paganelli et al [9] compare power control strategies for a parallel hybrid car, based on minimizing fuel consumption and the equivalent electric motor fuel consumption. Delprat et al [10] propose a control of parallel hybrid power train which is the optimal control that splits the power between the engine and electric motor in order to minimize the fuel consumption. This strategy optimize the fuel consumption considering the the torque engine and the gear ratio. Musardo et al [8] present the Adaptive Equivalent Consumption Minimization Strategy (A-ECMS), which is an algorithm for hybrid electric vehicles that attempts to minimize the vehicle fuel consumption and the stored electrical energy. To prove its effectiveness, A-ECMS strategy is

Preprint submitted to 4th Annual Dynamic Systems and Control Conference.
Received March 23, 2011.

compared with Dynamic Programming (DP) and a non adaptive ECMS [9]. Koot et al [11] establish energy management strategies for HEV using dynamic programming and quadratic programming with Model Predictive Control (MPC), to minimize fuel consumption. Local optimization strategies, like generalized predictive control (GPC) are also used with small prediction horizons.

In this paper a new strategy to control the power flow in a parallel power train HEV is presented. In this configuration, shown in Fig. 1, the internal combustion engine (ICE) and the electric machine (EM) can directly supply their torque to the driven wheels through a planetary gear system[1].

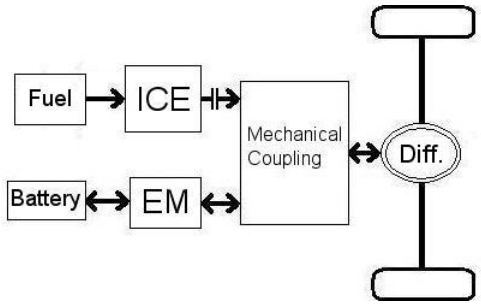

Figure 1. PARALLEL HYBRID ELECTRIC VEHICLE POWER-TRAIN.

The design of the strategy recognizes, as is also pointed out in Musardo et al [8], that optimization based solutions to HEV power flow control are very difficult to implement in real-time. Moreover, their results can not be as effective when real driving conditions differ from those used in the optimization problem solution. A similar problem occurs when the uncertainty in the models is considered.

The strategy in Musardo et al [8] proposes a local criterion to decide the power flow distribution and adapts a constant that determines the equivalent fuel consumption on the batteries during charge and discharge. In this paper a very different local criteria is used, that is based on the kinematic and dynamic constrains at the planetary gear system that must be satisfied when distributing the power demanded by the vehicle between the ICE and EM and in maximum efficiency curves for the ICE. There are only two pairs of parameters to tune that, as it will be shown later, have a similar behavior regardless of the driving cycle employed in the simulations.

To test the developed strategy, simulations of a mathematical model of the main components of the hybrid power-train which includes the ICE and EM, clutch, planetary gear system and battery were performed. The strategy was tested using three standard driving cycles for a bus in Mexico City.

The rest of paper is organized as follows. Section 2 presents the models for the vehicle subsystems, section 3 describes the controller for each power source, the driving cycles and details the continuos strategy for power flow control. Simulation results are presented in the section 4 while section 5 presents the conclusions and directions for future work.

[1]More details about HEV architectures can be found, for exampe, in [2]

HEV MODELING

Internal combustion engine model

The model is taken from [12]. It is assumed that the air entering the intake manifold follows the ideal gas law and that the manifold temperature varies slowly with respect to pressure and engine speed. The model is described by

$$\frac{d\omega_{ice}}{dt} = \frac{h_1}{\omega_{ice}}\dot{m}_f + h_2 p_a + \frac{h_3}{\omega_{ice}}P_b + \frac{h_4}{\dot{m}_f} \qquad (1)$$
$$\frac{dp_a}{dt} = h_5\dot{m}_{ai} - h_6\omega_{ice}p_a$$

where ω_{ice} the engine speed, $\dot{m}_f$ the fuel flow rate and is used as control signal, p_a the intake manifold pressure, $\dot{m}_{ai}$ air flow entering the manifold and P_b the total brake power. Terms h_j are constants determined to parted of model of [12].

Battery model

In the HEV, batteries are used as a temporary energy source that helps saving fuel and reducing emissions. The state of charge of the battery (*soc*) is defined as a measure of the amount of electrical energy stored in it. It is analogous to the fuel gauge in the tank. From [13] the (*soc*) of the battery is obtained from the expression

$$soc(t) = \min\{100, \max\{0, \frac{Q_0 - \int_{t_0}^{t} I_b(\tau)d\tau}{Q_t} \times 100\}\} \qquad (2)$$

where $I_b(t)$ is the discharging current; $\int_{t_0}^{t} I_b(\tau)d\tau$ the charge delivered by the battery; Q_0 the initial charge in battery and Q_t denoting the total charge the battery can store. The dynamic equations that describe the circuit model in Fig. 2 for discharging and charging are

$$\dot{V}_p = -V_p\frac{1}{R_dC} + V_o\frac{1}{R_dC} - I_b\frac{1}{C}, \quad si \qquad V_p \le V_o \qquad (3)$$
$$\dot{V}_p = -V_p\frac{1}{R_cC} + V_o\frac{1}{R_cC} - I_b\frac{1}{C}, \quad si \qquad V_p > V_o \qquad (4)$$

where the current $I_b = \frac{V_p - V_b}{R_b}$ is considered to have positive sign when the battery is discharging.

Electrical machine model

The EM is an induction motor that can operate as motor or generator. When operating as motor, it draws power from the battery and the output torque drives the wheels, in possible combination with the ICE torque. Functioning as generator, it can recover kinetic energy from regenerative braking, or take energy

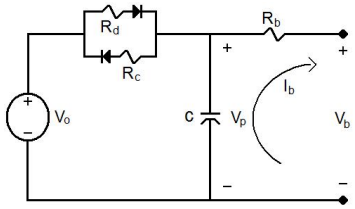

Figure 2. EQUIVALENT BATTERY CIRCUIT MODEL.

from the ICE to battery recharge. The model, obtained from [14], is

$$\begin{aligned}
\frac{d\omega}{dt} &= \frac{n_p L_m}{J L_r}(\psi_{rd} i_{sq} - \psi_{rq} i_{sd}) - \frac{1}{J} T_L - \frac{f}{J}\omega \\
\frac{d\psi_{rd}}{dt} &= -\frac{R_r}{L_r}\psi_{rd} + \frac{L_m}{L_r} R_r i_{sd} + (\omega_s - \omega)\psi_{rq} \\
\frac{d\psi_{rq}}{dt} &= -\frac{R_r}{L_r}\psi_{rq} - (\omega_s - \omega)\psi_{rd} + \frac{L_m}{L_r} R_r i_{sq}
\end{aligned} \tag{5}$$

$$\begin{aligned}
\frac{di_{sd}}{dt} &= -\left(\frac{R_s R_r}{\sigma L_s} + \frac{L_m^2 R_r}{\sigma L_s L_r^2}\right) i_{sd} + \omega_s i_{sq} \\
&\quad + \frac{L_m R_r}{\sigma L_s L_r^2}\psi_{rd} + \frac{L_m}{\sigma L_s L_r}\omega\psi_{rq} + \frac{1}{\sigma L_s} v_{sd} \\
\frac{di_{sq}}{dt} &= -\left(\frac{R_s R_r}{\sigma L_s} + \frac{L_m^2 R_r}{\sigma L_s L_r^2}\right) i_{sq} - \omega_s i_{sd} \\
&\quad - \frac{L_m}{\sigma L_s L_r}\omega\psi_{rd} + \frac{L_m R_r}{\sigma L_s L_r^2}\psi_{rq} + \frac{1}{\sigma L_s} v_{sq}
\end{aligned}$$

with $\sigma = 1 - \left(\frac{L_m^2}{L_s L_r}\right)$. The state variables for the EM are the speed, rotor fluxes and stator currents, $(\omega, \psi_{ra}, \psi_{rb}, i_{sa}, i_{sb})$, ω_s the synchronous electrical angular speed, J the induction motor inertia, n_p the number of pole pairs, L_m the magnetizing inductance, L_r the rotor inductance, T_L is the load torque, f the friction, R the resistance and v the voltage.

Planetary gear system

The coupling of the power sources to traction is accomplished through a planetary gear system (PGS). Fig. 3 shows a schematic of this mechanical device. The ICE is connected through a clutch-brake to the sun gear of the PGS, the EM is connected to the ring gear and the wheels are connected to the carrier gear ([15], [16]).

The gear ratio is calculated from the speed of the planet carrier with respect to the ring gear and sun gear, which is equivalent to a division of the radius of the ring gear between the radius of the sun gear. From [17] and [1],

$$R = \frac{\omega_s - \omega_p}{\omega_a - \omega_p} = -\frac{r_a r_p}{r_p r_s} = -\frac{r_a}{r_s} = -\frac{z_a}{z_s}$$

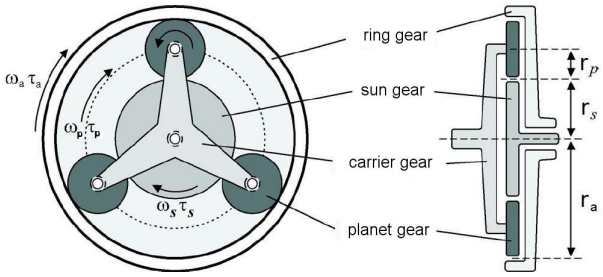

Figure 3. PLANETARY GEAR SYSTEM.

where ω is the angular velocity r the radius, z the number of theeth and subscripts s, p y a represent the sun, planet carrier and ring gear, respectively. Defining $k = r_a/r_s = -R$, the angular velocities in the PGS satisfy

$$\omega_p = \frac{1}{(k+1)}\omega_s + \frac{k}{(k+1)}\omega_a \tag{6}$$

where ω_p, ω_s and ω_a are the angular velocities of the planet carrier, ICE and EM.

The balance of power in the PGS satisfies

$$T_p\omega_p = T_s\omega_s + T_a\omega_a \tag{7}$$

Eqs. (6) and (7) are the kinematic and dynamic constraints, respectively, that any power flow strategy that employs a PGS must satisfy at all times.

Clutch system

To disengage the ICE from the sun gear of the PGS a clutch is included (see Fig. 4). Three modes of operation for the clutch

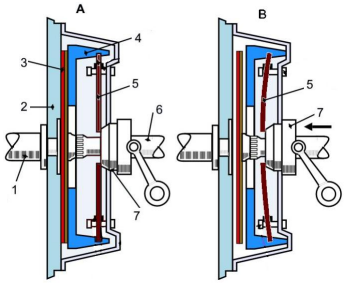

Figure 4. CLUTCH SYSTEM.

are modeled: when the ICE is disengaged, sliding and engaged ([18], [19]).

The clutch is modeled by

$$(J_{ice} + J_{clu})\dot{\omega}_{ice} = T_{ice} - T_{clu} - T_f \tag{8}$$

where J is the inertia, ω the velocity, T the torque, subscripts *ice*, *clu* and f are for ICE, clutch and friction, respectively. When the clutch is disengaged, $T_{clu} = 0$. When is slipping,

$$\begin{aligned} T_{clu} = [k_{e1} \int (\mid \omega_{ice} - \omega_{clu} \mid) dt] \times \\ [\mid (\omega_{ice} - \omega_{clu}) \mid (-0.0005) + 1] \times \\ f(\mid \omega_{ice} - \omega_{clu} \mid) \end{aligned} \tag{9}$$

where, k_{e1} is the stiffness coefficient of sliding.

Finally, when the clutch is engaged $\omega_{ice} = \omega_{clu}$ and

$$\begin{aligned} T_{clu} = k_{e2}(\int (\omega_{ice} - \omega_{clu}) dt) + \\ f_{es}(\omega_{ice} - \omega_{clu}) \end{aligned} \tag{10}$$

where k_{e2} is a stiffness coefficient, f_{es} an absorption coefficient.

Vehicle model

Vehicle is modeled like a moving mass subjected to a traction force $F_{tr}(t)$. The forces at the power-train also include the aerodynamic drag force $F_a(t)$, the rolling resistance $F_r(t)$ of the tires and the gravitational force $F_g(t)$ induced by the slope in the road, that are given by ([5], [17])

$$\begin{aligned} F_a(t) &= 0.5 \rho_a v(t)^2 C_d A_d \\ F_r(t) &= mg C_r \cos\gamma(t) \\ F_g(t) &= mg \sin\gamma(t) \end{aligned} \tag{11}$$

where ρ_a is the air density, $v(t)$ the vehicle speed, C_d the aerodynamic drag coefficient, A_d the vehicle frontal area, m the vehicle mass, g the gravity acceleration constant, C_r the tire rolling resistance coefficient and γ the road slope.

The vehicle velocity $v(t)$ is evaluated with

$$m \frac{dv(t)}{dt} = F_{tr} - F_a(t) - F_r(t) - F_g(t) - F_d(t) \tag{12}$$

that includes a force $F_d(t)$ to model perturbations and disturbances.

The drive-train torque $T_p(t)$ and the rotational speed $\omega_p(t)$ in the parallel architecture are obtained by taking into account the wheel radius r_{ll}, the final drive ratio R_f and the gear ratio K as ([17])

$$\begin{aligned} \omega_p(t) &= \frac{R_f}{r_{ll}} K v(t) \\ T_p(t) &= \frac{r_{ll}}{R_f} \frac{1}{K} F_{tr}(t) \end{aligned} \tag{13}$$

The mechanical power P_p demanded from the power train is

$$P_p(t) = \omega_p(t) T_p(t) = v(t) F_{tr}(t) \tag{14}$$

POWER FLOW CONTROL STRATEGY

It is assumed that the ICE and EM are controlled with two independent controllers, whose set points must be determined by power flow control strategy.

Diesel Engine Control

To control the speed of the diesel engine to a reference value $\omega_{ref} > 0$, the controller from [12] is used, that sets the fuel rate as

$$\dot{m}_f = \frac{-(h_2 p_a + \frac{h_3}{\omega_{ice}} P_b + \omega - \omega_{ref}) + \sqrt{\Delta h}}{2 \frac{h_1}{\omega_{ice}}} \tag{15}$$

where $\Delta_h = (h_2 p_a + \frac{h_3}{\omega_{ice}} P_b + \omega - \omega_{ref})^2 - 4 \frac{h_1}{\omega_{ice}} h_4$, for all $\omega(0) > 0$, verifies $\omega(t) \to \omega_{ref}$ when $t \to +\infty$. This control allows asymptoticly stable tracking of the ICE reference speed.

Control of induction motor

To control the EM, the sliding mode controller from [14] is used to set the voltages at the EM stator that allow to obtain asymptotic tracking of reference velocity and torque for the EM.

$$\begin{bmatrix} v_{sq} \\ v_{sd} \end{bmatrix} = -D^{-1} F - D^{-1} \begin{bmatrix} K_\omega & 0 \\ 0 & K_\psi \end{bmatrix} \begin{bmatrix} sign(S_{c1}) \\ sign(S_{c2}) \end{bmatrix} \tag{16}$$

where $K_\omega > 0$, $K_\psi > 0$. And

$$D = \frac{1}{\sigma L_s} \begin{bmatrix} -\frac{n_p^2 L_m}{J L_r} \psi_{rd} & 0 \\ 0 & -\frac{R_r L_m}{L_r} \end{bmatrix}, \qquad F = \begin{bmatrix} F_1 \; F_2 \end{bmatrix}^T$$

$$\begin{aligned} F_1 &= (\ddot{\omega}_{ref} + \lambda_\omega \dot{\omega}_{ref} + \frac{n_p}{J} \dot{T}_L) + (-\lambda_\omega + \frac{f}{J}) f_1 \\ &\quad - \frac{n_p^2 L_m}{J L_r} (i_{sq} f_2 + \psi_{rd} f_4) \\ F_2 &= (\ddot{\psi}_{rref} + \lambda_\psi \dot{\psi}_{rref}) + (\frac{R_r}{L_r} - \lambda_\psi) f_2 - \frac{R_r L_m}{L_r} f_3 \end{aligned}$$

Driving cycle

The driving cycles for Mexico City public transportation buses were obtained by West Virginia University [20]. There are three driving cycles with a duration of 1000 s. Fig. 5 shows the high speed driving cycle.

Strategy for power distribution

The control problem to be solved is to distribute the power required at PGS between the two power sources with the goal of saving fuel. This problem has multiple solutions, since many combinations of torque and speed at each power source can yield the demanded power.

The equations that constraint the solution of this problem are:

$$P_p = T_{em} \omega_{em} + T_{ice} \omega_{ice} = P_{em} + P_{ice} \tag{17}$$

Preprint submitted to 4th Annual Dynamic Systems and Control Conference.
Received March 23, 2011.

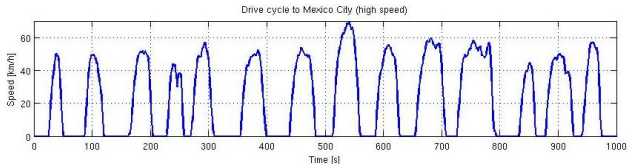

Figure 5. HIGH SPEED DRIVING CYCLE FOR A BUS IN MEXICO CITY.

$$\omega_p = \frac{1}{(k+1)}\omega_{ice} + \frac{k}{(k+1)}\omega_{em} \tag{18}$$

where P is power, T torque, ω speed and k the PGS gear ratio. Subscripts p, ice and em represent the planet carrier, ICE and EM, respectively. Note that P_p is the power required by the traction of the vehicle to meet the driving cycle requirements,.

The approach developed in this paper is based in the following observations:

1. The most important requirement in HEV power flow control is the ability to satisfy driver requirements.
2. All optimal solutions to power flow control preserves the state of charge of batteries, averaging over a long enough period time.
3. To minimize fuel consumption, ICE must be operated at high efficiency regions.

Observation 2, key in this paper strategy, is easily confirmed by noticing that all optimal solutions based on driving cycles must preserve the initial state of charge on the batteries at the end of cycle, otherwise the vehicle can not sustain a repetition of the same driving cycle. A similar observation is also made in Musardo et al [8], when discussing the tuning of A-ECMS. Observation 3 can be verified, for example, in [1] or [2], and it is one of the main reasons HEV are overall more efficient that normal vehicles.

There are two strategies for reducing fuel consumption: use the EM as much as possible and operate the ICE at the maximum possible efficiency.

Assuming that a reference state of charge in the batteries must be kept at a reference value, the first strategy for the traction case, $P_p > 0$, is accomplished by maximizing

$$J_1 = \max \int_0^{T_c} (sign(P_p) sign(soc - soc_{ref}) P_{em}\, dt \tag{19}$$

where T_c is the duration of the driving cycle, soc_{ref} is the reference value for soc and P_{em} the power at the EM. the power at the EM. This expression is useful for the cases of traction and traction-recharging batteries.

For the braking case, $P_p < 0$, the criteria is

$$J_2 = \max \int_0^{T_c} (sign(P_p) P_{em})\, dt \tag{20}$$

The value of Eqs. (19)-(20) is maximized when $P_{me} = \min\{sign(P_p)P_p, sign(P_p)P_{em}^{max}\}$, with P_{em}^{max} the maximum power attainable by the EM (assumed equal for the motor and generator cases). To avoid the switching induced by $sign(P_p)$ a smooth function of the soc is used. Therefore

$$P_{me} = P_{me}(soc) = \alpha_i(soc) P_{me}^{max} \tag{21}$$

where subindex in Eq. (21) is 1 when $P_p > 0$ and 2 when $P_p < 0$, $\alpha_i \in [-1, 1]$.

Assuming that P_p and ω_p are known, the proposed solution to the power flow control starts by substituting Eq. 21 in Eq. (17), that leads to

$$P_p = \alpha P_{em}^{max} + P_{ice} \tag{22}$$

The value of α_i is dependent on the reference value soc_{ref}

The shape of $\alpha_i(soc)$ determines how much electric power is taken or provided at a given point. One possible choice for $\alpha_i(soc)$ is shown in Fig. 6 that is described by

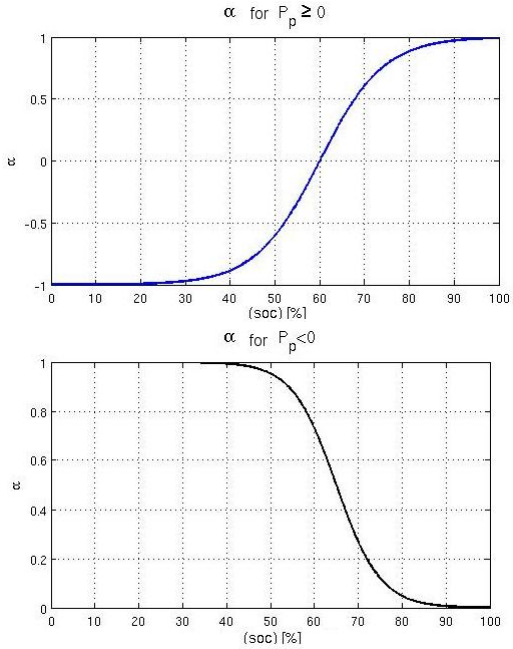

Figure 6. α_i FOR $P_p \geq 0$ AND $P_p < 0$.

$$\alpha_1 = \tanh(A_1(soc - soc_{ref})) \qquad P_p \geq 0 \tag{23}$$

$$\alpha_2 = 0.5 - 0.5(\tanh(A_2(soc - soc_{full}))) \quad P_p < 0 \tag{24}$$

where soc_{full} is a reference value to avoid battery overcharging in the generator case.

Preprint submitted to 4th Annual Dynamic Systems and Control Conference.
Received March 23, 2011.

Fig. 6 reveals that when $P_p \geq 0$, $\alpha_1 \in [-1,1]$ depending on the state charge of the battery; if α_1 is positive the EM operates as motor, otherwise it operates as generator. When $P_p < 0$, $\alpha_2 \in [0,1]$, regenerative braking is possible and the EM can work only as generator. This choice allows to make maximum use of electric power for traction or recharging of the batteries.

With α_i chosen, electric power in Ec.(17) is fixed. P_{ice} is determined as follows:

$$P_{ice} = min(P_p - P_{em}, P_{ice}^{max}); \quad P_p \geq 0$$

that guarantees that the ICE provides power below its maximum available power P_{ice}^{max}.

For the case of regenerative braking, $P_p < 0$, the generator has a limit in the recovered power and therefore

$$P_{brake} = \max\{0, P_p - \alpha_2 P_{em}^{max}\}$$

where P_{brake} is the power dissipated in the friction brakes.

Given P_{ice}, the angular velocity at which the ICE must operate, ω_{ice}, is obtained from the maximum efficiency curve in the power vs. angular velocity curve. This curve has a shape similar to that shown in Fig. 7 and is approximated by a polynomial with P_{ice} as independent variable. With this choice, it is assured that the ICE is always used with maximum efficiency.

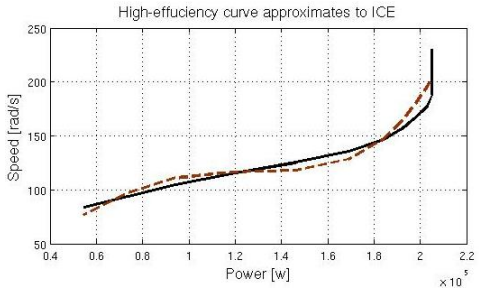

Figure 7. POWER VS. SPEED HIGH EFFICIENCY CURVE OF THE ICE.

Once ω_{ice} is obtained from the maximum efficiency curve, the required torque in the ICE is obtained from

$$T_{ice} = \frac{P_{ice}}{\omega_{ice}} \qquad for \qquad \omega_{ice} > 0 \tag{25}$$

$$T_{ice} = 0 \qquad for \qquad \omega_{ice} = 0 \tag{26}$$

The final step is to determine the angular velocity and torque for the EM. From Eq. (18) ω_{em} is

$$\omega_{em} = \frac{(k+1)}{k}(\omega_p - \frac{1}{(k+1)}\omega_{ice}) \tag{27}$$

and the torqueT_{em} is derived from

$$T_{em} = \frac{P_{em}}{\omega_{em}} \qquad for \qquad \omega > 0 \tag{28}$$

$$T_{em} = 0 \qquad for \qquad \omega = 0 \tag{29}$$

In the case of regenerative braking, $P_p < 0$ and $P_{ice} = 0$ and the recovering of the electric power follows directly.

SIMULATION RESULTS.

Simulations were carried out for a bus with mass of 15,000 $[kg]$, a diesel ICE of 205 $[kw]$, a clutch between the ICE and a PGS with $k = 5$. The electric machine is a induction motor of 93 $[kw]$ and the batteries are $25[Ah]$ at $288[V]$. The bus is commanded to follow the three standard driving cycles: low velocity (1), medium velocity (2) and high velocity (3).

There are four parameters to tune in the algorithm: A_1, A_2, soc_{ref} and soc_{full}. Additionally, the initial state of charge of the batteries, soc_{in}, must be considered. Extensive simulations were executed to test the sensitivity of the strategy to these parameters and to find the best combination of them. Findings are summarized below. All the reported simulations have in common that the initial state of charge soc_{in} and the final state of charge soc_{fin} of the batteries were almost equal. Combination of parameters that violated this condition were discarded.

As mentioned, the most important feature of any power flow control strategy in HEV is the ability to track driver demands.Typical examples of speed tracking capability are shown in Figs. 8 and Fig. 9, that illustrate desired and real velocity of the HEV and the speed tracking error, for the high and medium speed driving cycles, respectively. Peak errors are $2[km/h]$ and medium speed error tracking is about $0.25[km/h]$. These errors are very acceptable and within the margin of errors reported in the literature.

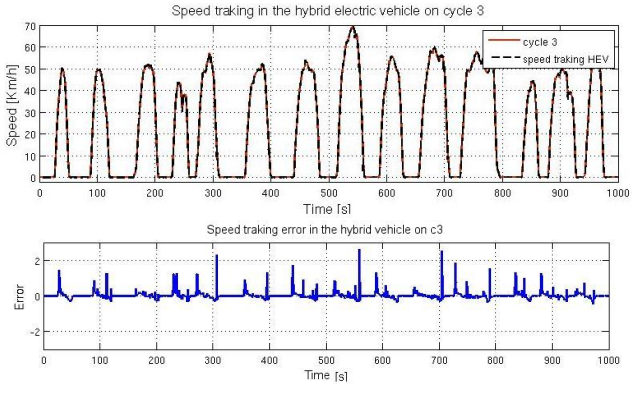

Figure 8. SPEED TRACKING OF THE HEV FOR HIGH SPEED DRIVING CYCLE (3).

Tables 1-3 show the most significant results on the tuning of the algorithm[2]. The initial state of charge of the batteries is

[2]For comparison purposes consider that the fuel consumption for the three

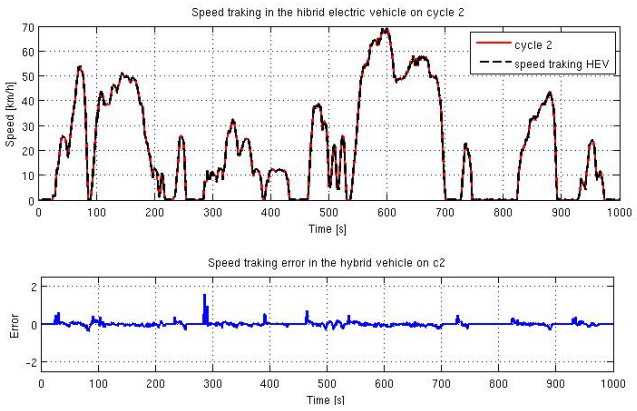

Figure 9. SPEED TRACKING OF THE HEV FOR MEDIUM SPEED DRIVING CYCLE (2).

chosen in such a way that

$$soc_{ref} < soc_{in} < soc_{full}$$

The value of soc_{ref} was established at 60% for most cases and to 70% for the rest. This value is not particularly important as it is more related to the desired autonomy of the HEV when only the EM can operate. The difference $soc_{full} - soc_{ref}$ and $soc_{in} - soc_{ref}$ is what is most important. For a given choice of soc_{in} and soc_{full} different values of A_1 and A_2 were tried in such a way that a full excursion between $[-1,1]$ and $[0,1]$, respectively, was possible.

The role of soc_{full} is to incentive energy recovering during regenerative braking. It was found that when $soc_{full} - soc_{in} > 10\%$, no additional energy was recovered in the regenerative braking for all cycles. Larger values of A_2, that produce a more abrupt transition in α_2, have no additional effect as the soc_{in} was well bellow the zone when transitions occurs. On the other hand, this larger values allows to appropriately handle situations when the initial state of charge is very high.

The role of A_1 is also unveiled by the results. Very low values of A_1 do not encourage the use of the EM. Larger values can only be used with smaller differences between soc_{ref} and soc_{in}.

It is very interesting to note that the same set of parameters produced the same best results for all three driving cycles. This is in contrast with the strategy presented in Musardo et al [8], that requires different reference values for each driving cycle.

Fig. 10 shows simulation results for different battery capacities with the same soc_{in}. It is clear that the size of the oscillations increases for smaller batteries. This indicates that a smaller size of the battery pack is feasible and that in HEV's the size of the pack is more related with the desired autonomy than with the role in the driving cycle.

driving cycles for a bus with only ICE are 17.36, 10.13 and 8.95$[kg]$, for the high, medium and low speed driving cycles, respectively

Table 1. HIGH SPEED DRIVING CYLCE (3). VARIATION OF PARAMETERS A_1, A_2, soc_{ref} AND soc_{in} VS. TOTAL FUEL CONSUMPTION $[kg]$.

A_1	soc_{ref}	A_2	soc_{full}	Fuel	soc_{in}	soc_{fin}
0.040	60	0.13	65	10.65	63.5	63.57
0.055	60	0.13	75	10.21	63.5	63.57
0.055	60	0.30	90	10.21	63.5	63.57
0.085	70	0.30	90	10.20	72.3	72.35

Table 2. MEDIUM SPEED DRIVING CYCLE (2). VARIATION OF PARAMETERS A_1, A_2, soc_{ref} AND soc_{in} VS. TOTAL FUEL CONSUMPTION $[kg]$.

A_1	soc_{ref}	A_2	soc_{full}	Fuel	soc_{in}	soc_{fin}
0.040	60	0.13	65	8.986	63.5	63.4
0.055	60	0.13	75	8.653	63.5	63.43
0.055	60	0.30	90	8.653	63.5	63.43
0.085	70	0.30	90	8.652	72.3	72.24

Table 3. LOW SPEED DRIVING CYCLE (1).VARIATION OF PARAMETERS A_1, A_2, soc_{ref} AND soc_{in} VS. TOTAL FUEL CONSUMPTION $[kg]$.

A_1	soc_{ref}	A_2	soc_{full}	Fuel	soc_{in}	soc_{fin}
0.040	60	0.13	65	7.558	63.5	63.51
0.055	60	0.13	75	7.36	63.5	63.56
0.055	60	0.30	90	7.36	63.5	63.55
0.085	70	0.30	90	7.353	72.3	72.34

CONCLUSIONS

A new strategy for power flow control that allows to distribute the power at the planetary gear system of a parallel HEV was presented. The strategy satisfies driver requirement and focuses in maximizing the use electric machine to provide traction power or recharging the batteries with the aim of preserving the state of charge of the batteries and to operate the internal combustion engine at the maximum possible efficiency.

The strategy was developed using the dynamic and kinematic constraints at the planetary gear system and avoids the commutation of power sources normally found in other approaches for energy management in HE. The strategy developed is simple and implicitly includes the results of optimum control based strategies when forcing the ICE to function in the high-

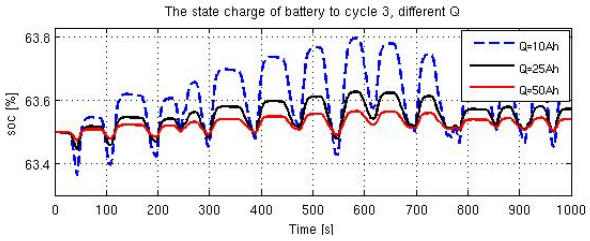

Figure 10. VARIATION OF *soc* FOR DIFFERENT BATTERY PACK CAPACITIES.

efficiency regions to reduce fuel consumption.

To test the strategy, numerical simulations of a mathematical model of the HEV that included the internal combustion engine, electric engine, planetary gear system, clutch and transmission were carried out. Simulation results for a diesel HEV were obtained that show that the strategy achieves small velocity tracking errors, is easy to tune when compared with other approaches available in the literature while obtaining similar fuel savings. An adaptive version of the strategy and experimental testing of the strategy is ongoing work.

ACKNOWLEDGEMENT

This research was supported by CONACYT grant 103640 and UNAM-PAPIIT grant IN108010. The first two authors specially acknowledge the support from CONACYT scholarship program.

REFERENCES

[1] John. M. Miller, 2006. "Hybrid Electric Vehicle Propulsion System Architectures of the e-CVT Type". *IEEE Transactions on Power Electronics,* **21**, May, pp. 756–767.

[2] Ehsani, M., Gao, Y., and Miller, J. M., 2007. "Hybrid Electric Vehicles: Architecture and Motor Drives". *Proceedins of the IEEE,* **95**, April, pp. 719–728.

[3] Pisu, P., and Rizzoni, G., 2007. "A Comparative Study Of Supervisory Control Strategies for Hybrid Electric Vehicles". *IEEE Transactions on Control Systems Technology,* **15**, may, pp. 506–518.

[4] Chau, K. T., and Chan, C. C., 2007. "Emergin energy-efficient technologies for hybrid electric vehicles". *Proceedins of the IEEE,* **95**, April, pp. 821–835.

[5] Xiong, W., Zhang, Y., and Yin, C., 2009. "Optimal Energy Management for a Series-Parallel Hybrid Electric Bus". *Energy conversion and management,* **50**, July, pp. 1730–1738.

[6] Tzeng, S., Huang, K. D., and Chen, C. C., 2005. "Optimization of the dual energy-integration mechanism in a parallel-type hybrid vehicle". *Applied Energy,* **80**, pp. 225–245.

[7] Xiong, W. W., and Yin, C. L., 2009. "Design of series-parallel hybrid electric propulsion systems and application in city transit bus". *WSEAS Transaction on Systems,* **8**, May, pp. 578–590.

[8] Musardo, C., Rizzoni, G., and Sataccia, B., 2005. "A-ecms: An adaptive algoritm for hybrid electric vehicle energy management". In 44th IEEE Conference on Decicsion and Control, and the European Control Conference, pp. 1816–1823.

[9] Paganelli, G., Guerra, T. M., Delprat, S., Santin, J.-J., Delhom, M., and Combes, E., 2000. "Simulation and assessment of power control strategies for a parallel hybrid car". *Journal of automobile engineering,* **214**, pp. 705–717.

[10] Delprat, S., Lauber, J., Guerra, T. M., and Rimaux, J., 2004. "Control of a parallel hybrid powertrain: Optimal control". *IEEE Transactions on Vehicular Technology,* **53**, May, pp. 872–881.

[11] Koot, M., Kessels, J. T. B. A., de Jager, B., Heemels, W. P. M. H., van den Bosch, P. P. J., and Steinbuch, M., 2005. "Energy management strategies for vehicular electric power systems". *IEEE Transactions on Vehicular Technology,* **54**, May, pp. 771–782.

[12] Outbib, R., Dovifaaz, X., Rachid, A., and Ouladsine, M., 2002. "Speed control of a diesel engine: a nonlinear approach". In American Control Conference, pp. 3293–3294.

[13] Chiasson, J., and Vairamohan, B., 2005. "Estimating the State of Charge of a Battery". In Control Systems Technology, Vol. 13, pp. 465–470.

[14] Mezouar, A., Fellah, M. K., Hadjeri, S., and Sahali, Y., 2006. "Adaptive speed sensorless vector control of induction motor using singularly perturbed sliding mode observer". *IEEE Industrial Electronics*, Nov 6-10, pp. 932–939.

[15] Ambarisha, V. K., and Parcker, R. G., 2007. "Nonlinear dynamics of planetary gears using anlytical and finite element models". *Journal of sound and vibration,* **302**, January, pp. 577–595.

[16] Szumanowski, A., Yuhua, C., and Piórkowski, P., 2005. "Analysis of Different Control Strategies and Operating Modes of Compact Hybrid Planetary Transmission Drive". *Vehicle Power and Propulsion,* **7**, sept, pp. 673–680.

[17] Kessels, J. T. B. A., Koot, W. T., van den Bosch, P. P. J., and Kok, D. B., 2008. "Online Energy Management for Hybrid Electric Vehicles". *IEEE Transactions on Vehicular Technology,* **57**, november, pp. 3428–3440.

[18] Powell, B. K., Bailey, K. E., and Cikanek, S. R., 1998. "Dynamic modeling and control of hybrid electric vehicle powertain systems". *IEEE Control Systems*, October, pp. 17–33.

[19] James, D., and Narasimhamurthi, N., 2005. "Design of a optimal controller for commercial trucks". In American Control Conference, pp. 1599–1606.

[20] Vega, E., 2006. "Pruebas en Campo de Autobuses de Tecnologías Alternativas en la Ciudad de México". *Gobierno del Distrito Federal, Secretaría del Medio Ambiente*, Mayo, pp. 30–32.